Forced Molecular Rotation in an Optical Centrifuge

D. M. Villeneuve,[1,*] S. A. Aseyev,[1] P. Dietrich,[1,2] M. Spanner,[1] M. Yu. Ivanov,[1] and P. B. Corkum[1]

[1]*National Research Council of Canada, 100 Sussex Drive, Ottawa, Ontario, Canada K1A 0R6*

[2]*Freie Universität Berlin, Arnimallee 14, D-14195 Berlin, Germany*

(Received 17 February 2000)

Intense linearly polarized light induces a dipole force that aligns an anisotropic molecule to the direction of the field polarization. Rotating the polarization causes the molecule to rotate. Using femtosecond laser technology, we accelerate the rate of rotation from 0 to 6 THz in 50 ps, spinning chlorine molecules from near rest up to angular momentum states $J \sim 420$. At the highest spinning rate, the molecular bond is broken and the molecule dissociates.

PACS numbers: 33.80.Ps, 42.65.Re

It has recently been predicted that diatomic molecules can be rotationally accelerated from rest up to the point where the molecular bond is torn apart by the centrifugal force [1], in less than one ground state rotational period. In this process, a molecule has to undergo several hundred successive Raman transitions up the ladder of rotational states, each in a fraction of a picosecond and with nearly 100% probability. To achieve such high efficiency, the laser intensity must be high enough to force the transition, and the frequency content of the laser pulse must constantly change to match the changing Raman transition energy. This can be accomplished using femtosecond laser technology which gives precise control over the amplitude, phase, frequency, and polarization of the laser radiation.

We will demonstrate that we can rotationally accelerate Cl_2 molecules up to the point where the molecular bond is broken by the centrifugal force. We use either a rotationally cold or nearly room-temperature ensemble. In the experiment, angular traps with depths of 50–100 meV, exceeding room temperature, were achieved for Cl_2 with minimal ionization during the 50 ps pulse.

Our experiment relates to several directions in modern atomic and molecular physics. It is the rotational analog of experiments on accelerating cold atoms in optical lattices [2]. It is an example of chirped-pulse excitation schemes in multilevel systems [3], whereby we realize highly efficient chirped-pulse Raman excitation of the rovibrational system. By guiding the rotation of a molecule whose nuclear wave function is confined in three dimensions, we have created a molecular analog of Trojan wave packets [4] in atoms.

Forced rotation is a special case of strong-field molecular optics. Strong fields are a natural tool for molecular optics. Molecules have very complex spectra, making standard atomic cooling techniques with resonant light difficult. Cold molecules can be produced either by photoassociation [5] of cold atoms or using buffer gas cooling [6]. While cooling simplifies control over translational motion, complete control of rotations still requires deep angular traps. Strong nonresonant laser fields can create near room-temperature–deep traps for both rotational and translational motion, making cooling less critical. Nonresonant traps have been used to trap [7], focus, deflect [8], and align molecules [9]. Alignment was used to control simple unimolecular reactions via the vector properties of the transition [9].

The intention of the experiment is to demonstrate centrifugal dissociation. If instead we want to demonstrate efficient spinning of molecules, then we would choose a lighter molecule that better suits the energy capability of our laser system. Although spinning anisotropic molecules using the nonresonant dipole force is general, Cl_2 is an ideal candidate for a first experiment. Near the equilibrium internuclear separation, single photon absorption is not possible [see Fig. 1(a)] with an 800 nm photon—the frequency region where the most advanced femtosecond sources operate. In this region we have both exquisite control over the optical pulse and access to high intensities and, hence, very deep angular traps.

Figure 1(b) is a plot of the Cl_2 ground state potential for different angular momenta J. As J increases, the bond starts to stretch until it is lost near $J = 420$. Bond breaking requires a rotational frequency of almost 5 THz, well within the bandwidth of our Ti:sapphire laser pulse. It leads to clearly identifiable chlorine atom fragments with kinetic energy of $\sim$1 eV. In the experiment, a large fraction of the molecules was spun to dissociation in under one ground state rotational period (70 ps for Cl_2), starting from either cold or nearly room temperature rotational distribution.

Up to four laser beams were used, all split from a 5 mJ pulse produced by a 10 Hz Ti:sapphire laser system. The FWHM bandwidth of the pulse was over 30 nm with a central wavelength of 810 nm, compressible to 50 fs, and stretched to a duration of 50 ps before amplification; the stretching resulted in a positive frequency chirp.

Two beams were used to make an optical centrifuge [1], a pulse with rotating linear polarization that spins the molecules. Such rotation, at frequency Ω, is accomplished by combining two counterrotating circularly polarized fields with frequencies $\omega_L - \Omega$ and $\omega_L + \Omega$. To increase Ω with time we chirp the two circularly polarized pulses in opposite frequency directions.

 0031-9007/00/85(3)/542(4)$15.00 © 2000 The American Physical Society

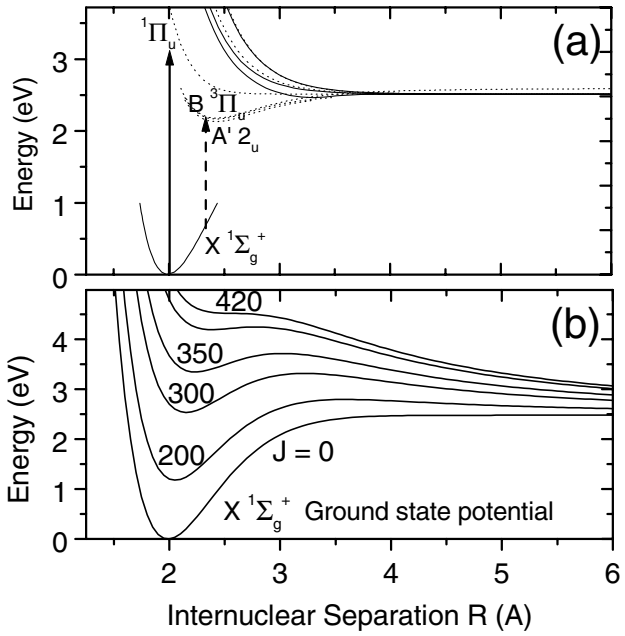

FIG. 1. (a) Potential energy diagram of Cl_2 showing the ground state and the manifold of low-lying excited states. The 800 nm photons used for spinning have insufficient energy to electronically excite the molecule. A 400 nm photon can excite to the A and B states and initiate dissociation. (b) shows how the ground state potential changes with increases rotational quantum number J, leading to the bond breaking at $J \approx 420$. Excited states are modified to the same extent.

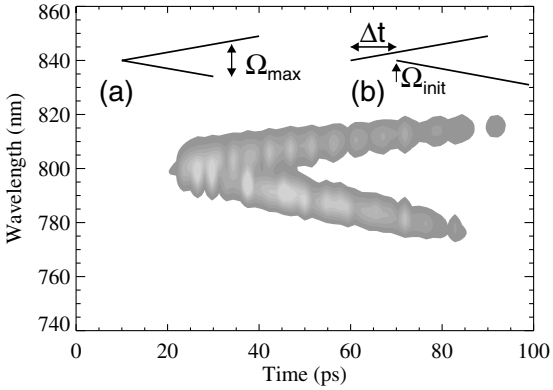

FIG. 2. Frequency resolved cross-correlation measurement of the two oppositely chirped laser beams that make the spinning pulse. The spectral widths are due to the width of the 50 fs, 800 nm pulse that was used for the cross correlation. The insets show figuratively how the pulses were manipulated to limit Ω_{max} and to increase Ω_{init}. (a) Normally, Ω_{max} is determined by the bandwidth of the femtosecond pulse that is used to generate the centrifuge. Ω_{max} can be controlled by truncating the spectrum of one of the pulses at the Fourier plane of the stretcher. (b) Ω_{init} is controlled by delaying one of the pulses, so that the polarization is already spinning when both pulses are on.

To accomplish this in practice, the stretched pulse was incident onto a stretcher composed of three 1200 line/mm gold gratings and three 150 mm focal length achromatic doublet lenses. Half of the spectrum was reflected by a dielectric mirror placed in the Fourier plane of one grating/lens pair, and the other half was transmitted to the other grating/lens pair. The long wavelength part traveled farther and so the chirp was inverted. Mirrors at the end of each arm controlled the relative timing of the pulses and returned each spectral component so that they recombined at the first grating, vertically displaced. The displacement allowed a $\lambda/2$ plate to be inserted in one beam. The two oppositely chirped, orthogonally polarized components were combined in a polarizer and passed through a $\lambda/4$ plate to make them left and right circularly polarized. In time, each pulse had a $\sim$2 ps rise time followed by a $\sim$50 ps falloff. The rising edges were coincident within 1 ps. Energies of up to 500 μJ were available in the centrifuge pulse inside the target chamber. Figure 2 shows the frequency resolved cross-correlation measurement of the optical centrifuge pulse.

The two counterrotating beams, along with two diagnostic pulses, were combined at beam splitters, superimposed in the near field, and then aligned in the far field using a long focal length mirror and a CCD camera. An optional 400 nm pulse (20 μJ, 2 ps) came approximately 200 ps after the spinning pulses and was used to dissociate the molecules. An ionizing pulse (800 nm, 15 μJ, 50 fs) came another 300 ps later and served to ionize any atoms or molecules so they could be detected in the time-of-flight system.

All beams were focused in a vacuum chamber with a 50 mm focal length on-axis parabolic mirror. The beam diameters were 8 μm FWHM for the optical centrifuge and 5 μm for the two diagnostic pulses, both polarized parallel to the time-of-flight axis.

The supersonic molecular beam emerged from a pulsed valve with a 100 μm diameter orifice located 12 cm from the focus. Chlorine gas at 150 mbar was mixed with 1.5 bars of neon buffer gas, giving an estimated rotational temperature of $\sim$10 K.

The time-of-flight mass spectrometer [8] had a 3 cm long acceleration region separated from a 3 cm field-free drift region by an 0.5 mm diam aperture. This geometry enabled the initial kinetic energy of fragments to be directly measured from the separation in time of two symmetric peaks with respect to the atomic mass center. The aperture reduces the collection efficiency of high energy fragments (since its acceptance angle is energy dependent) and of the fragments from spinning molecules (since they are distributed over 360°). Consequently, many more molecules are dissociated than is apparent from the magnitude of the signals in the figures below.

Figures 3(a)–3(c) show a portion of the mass spectrum around the arrival time for Cl^+, with only the spinning pulse and the 50 fs ionizing pulse (to ionize the fragments). The most prominent peak on the right of Figs. 3(a)–3(c) is produced by zero kinetic energy Cl_2^{2+}. This ion is quite stable since double ionization of Cl_2 by an 800 nm pulse

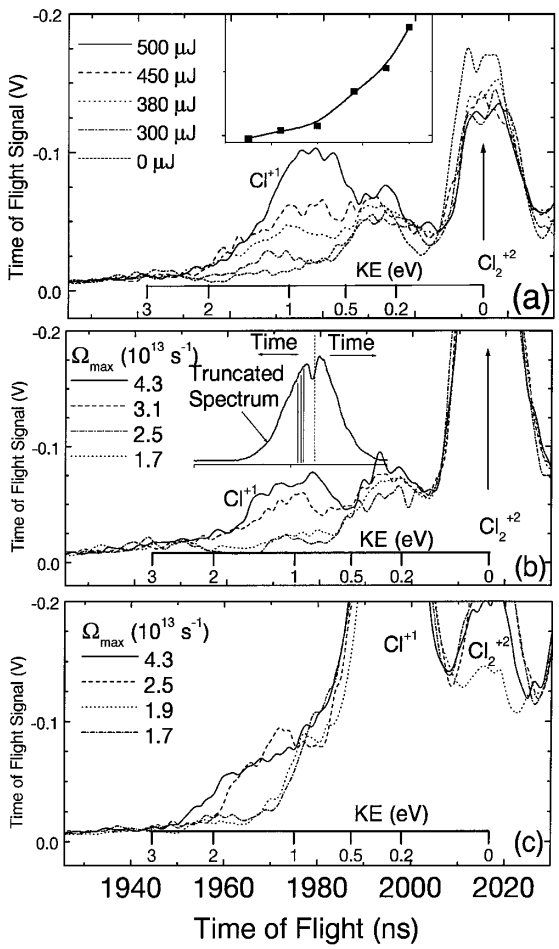

FIG. 3. Time-of-flight mass spectra of spinning chlorine molecules in the Cl^+ region. Translational energy of the fragments is determined from the arrival time. (a) The signal near 1 eV, corresponding to rotational dissociation, increases quickly with increasing energy of the centrifuge laser pulse. The inset shows how the integrated signal around 1 eV increases rapidly with laser energy. (b) Reducing the maximum spinning frequency Ω_{max} suppresses the signal near 1 eV; the threshold is at $\Omega_{max} \sim 2.6 \times 10^{13}$ s^{-1}, as expected. The inset shows how the spectrum was truncated to reduce Ω_{max}. (c) Mass spectrum with an additional delayed 400 nm 2 ps pulse, used to dissociate the rotating molecules and detect their rotational energy. This detects those molecules that are spinning but have not been dissociated by the centrifuge. As Ω_{max} is reduced, the maximum energy is similarly reduced, as expected.

removes antibonding electrons. We show only the region to the left of the $_{35,35}Cl_2^{2+}$ molecular isotope because on the right of the spectrum the atomic fragment peaks are masked by the $_{35,37}Cl_2^{2+}$ molecular isotope. A kinetic energy scale for the Cl^+ atoms is superimposed.

According to Fig. 1(b), rotational dissociation of Cl_2 should yield atomic fragments with kinetic energy $\sim$1 eV. Figure 3(a) shows that chlorine atom fragments around $\sim$1 eV are associated with the spinning pulse. The inset shows that this peak increases nonlinearly with intensity. These results are consistent with chlorine atoms being produced by the rotational dissociation of Cl_2: as the spinning angular potential well gets deeper, more and more molecules are spun to dissociation. We have obtained similar results without the buffer gas in the jet expansion, i.e., with rotationally hot molecules, although the spinning efficiency was somewhat reduced.

We made several tests to verify that the 1 eV peak in Fig. 3(a) is due to molecules being spun by the centrifuge until they dissociate. (1) When one of the two beams that make up the optical centrifuge was blocked or when the two beams were linearly polarized, no atomic fragments were seen. (2) We could reduce the maximum spinning frequency, Ω_{max}, by truncating in frequency one of the two optical centrifuge beams (Fig. 2 inset). As expected, the atomic fragments around 1 eV disappeared for $\Omega_{max} < 2.6 \times 10^{13}$ s^{-1} (4.2 THz), i.e., when Ω_{max} was insufficient to reach $J \sim 420$ [see Fig. 3(b)]. (3) The rotating angular trap could be turned on at higher initial spinning frequency, Ω_{init}, by delaying one of the two chirped circularly polarized pulses of the optical centrifuge (Fig. 2 inset). As shown in Ref. [1], for rotational temperatures much less than the angular well depth U_0, efficient angular trapping requires $I\Omega_{init}^2 < U_0$, where I is the moment of inertia. When $I\Omega_{init}^2 > U_0$, the angular trap is rotating too quickly to trap molecules at the time it is turned on. A delay of $\Delta t = 5$ ps reduced the signal by 50%, and for $\Delta t > 10$ ps the signal disappeared. Fully quantum-mechanical simulations using this Δt dependence yield $U_0 \sim 100$ meV, in excellent agreement with the estimate based on the quadratic Stark shift given by the intensity of the optical centrifuge beam.

Figures 3(a) and 3(b) clearly show that we can spin molecules until they dissociate. We must note, however, that, according to Fig. 1(a), as the molecule stretches to near dissociation, a single 800 nm photon transition (shown with the short arrow) becomes possible from the ground state to a manifold of weakly bound and dissociative electronic states. Hence, at the very last moment the rotational dissociation can be aided by a one-photon absorption. Nevertheless, even in this case $J \sim 400$ has to be reached and the molecule has to make almost 200 Raman transitions during the pulse (i.e., at a rate of about one transition per 200 fs). The most probable kinetic energy ($\sim$1 eV) is consistent with dissociation by the centrifuge; the higher cutoff is the energy expected for photon assisted dissociation.

More insight can be gained by using an additional 2 ps 400 nm probe pulse, delayed by 200 ps with respect to the centrifuge pulse. According to Fig. 1(a), a single 400 nm photon (shown with the long arrow) can dissociate Cl_2 by exciting it to the dense manifold of electronically excited states. Hence this 400 nm pulse gives us a method to detect spinning molecules by "cutting the bond" and converting the rotational energy into translational.

Figure 3(c) shows the time-of-flight spectrum obtained using all four pulses—pulses for spinning, dissociation,

and ionization. Molecules with no rotational energy lead to fragments with kinetic energy of about 0.3 eV, equal to the photon energy of 3.1 minus 2.5 eV dissociation energy for the two atoms. These are seen in the figure as the off-scale Cl^{+1} fragments. With the spinning pulse present, fragments with kinetic energies of up to ~2 eV were seen, while without the spinning pulse no energetic atoms are seen.

For this part of the experiment, we performed the same tests as described above, with similar results. For example, the maximum rotational frequency Ω_{max} was reduced by truncating the spectrum of one of the counter-rotating beams. Table I shows Ω_{max} and the corresponding range of cutoff energy of the fragments, calculated using the centrifugally modified potential energy surfaces in Fig. 1(b). The range of kinetic energies is due to the possible range of vibrational energy. E_{min} corresponds to excitation from the bottom of the potential, whereas E_{max} corresponds to excitation from the highest bound vibrational state of the well. The fact that we observe molecules spinning very close to the dissociation rate suggests that at least some of them are being spun with very little vibrational excitation.

Every measurement that we have performed is consistent with spinning Cl_2 in an optical centrifuge. We have also performed preliminary experiments with O_2 and CS_2. Our observations are consistent with successful spinning of these molecules, although the maximum spinning frequency achieved with our laser was not sufficient for rotational dissociation of the ground state.

These results have important implications for both chemistry and physics. From a gas phase chemistry perspective, we open a new pathway for photochemistry with molecules in extreme angular momentum states. This would be especially interesting for polyatomic molecules, where the centrifugal force modifies the much more complex potential energy surface. Huge changes in the electronic states are possible (see Fig. 1).

From a surface chemistry perspective, we can produce molecules with high J and M_J and direct them towards a surface. The rotational energy of such a molecule can be in the multi-eV range, sufficient to stimulate chemistry on the surface. When J control is combined with molecular focusing, a new experimental pathway for precision etching and surface studies will be opened.

From a physical perspective, this experiment shows that molecules are devices that can be manipulated with precision. All aspects of the spinning pulse are under our control, allowing us to control the time dependent molecular alignment. If the gas density is high enough, spinning molecules can serve as a precisely controlled high-frequency modulator with the modulation synchronizable with femtosecond precision. If the molecules have a dipole moment, they could provide an intense source of tunable multi-THz radiation.

TABLE I. Maximum rotating frequencies, and predicted range of cutoff kinetic energy of fragments, corresponding to the curves in Fig. 3(c). $\Omega_{max} > 2.6 \times 10^{13}$ s^{-1} is sufficient to dissociate chlorine with no vibrational excitation. Those molecules that are lost from the centrifuge before reaching Ω_{max} will produce lower kinetic energy fragments.

Ω_{max} (s^{-1})	E_{min} (eV)	E_{max} (eV)
4.3×10^{13}	2.2	2.5
2.5×10^{13}	1.7	2.1
1.9×10^{13}	1.0	1.7
1.7×10^{13}	0.9	1.7

We acknowledge fruitful discussions with P. H. Bucksbaum, M. Shapiro, G. Gerber, J. Karczmarek, K. Davitt, A. Stolow, and D. M. Rayner. We thank B. Avery for his continuing technical support.

*Email address: david.villeneuve@nrc.ca

[1] J. Karczmarek *et al.,* Phys. Rev. Lett. **82**, 3420 (1999).
[2] Q. Niu and M. G. Raizen, Phys. Rev. Lett. **80**, 3491 (1998).
[3] For theory, see, e.g., S. Chelkowski, A. D. Bandrauk, and P. B. Corkum, Phys. Rev. Lett. **65**, 2355 (1990); for experiments, see, e.g., B. Broers, H. B. van Linden van den Heuvell, and L. D. Noordam, Phys. Rev. Lett. **69**, 2062 (1992) (electronic ladder climbing); D. J. Maas *et al.,* Chem. Phys. Lett. **290**, 75 (1998) (vibrational ladder climbing).
[4] See, e.g., I. Bialynicki-Birula, M. Kalinski, and J. H. Eberly, Phys. Rev. Lett. **73**, 1777 (1994); A. F. Brunello, T. Uzer, and D. Farrelly, Phys. Rev. Lett. **76**, 2874 (1996).
[5] A. N. Nikolov *et al.,* Phys. Rev. Lett. **84**, 246 (2000); **82**, 703 (1999).
[6] J. D. Weinstein *et al.,* Nature (London) **395**, 148 (1998).
[7] T. Takekoshi, B. M. Patterson, and R. J. Knize, Phys. Rev. Lett. **81**, 5105 (1998); K. M. O'Hara *et al.,* Phys. Rev. Lett. **82**, 4204 (1999).
[8] H. Stapelfeldt *et al.,* Phys. Rev. Lett. **79**, 2787 (1997); H. Sakai *et al.,* Phys. Rev. A **57**, 2794 (1998).
[9] For first theoretical papers, see, e.g., B. Zon and B. Katsnelson, Zh. Eksp. Teor. Fiz. **69**, 1166 (1975) [Sov. Phys. JETP **42**, 595 (1976)]; B. Friedrich and D. Herschbach, Phys. Rev. Lett. **74**, 4623 (1995); for experiments, see, e.g., H. Sakai *et al.,* J. Chem. Phys. **110**, 10235 (1999); J. J. Larsen, I. Wendt-Larsen, and H. Stapelfeldt, Phys. Rev. Lett. **83**, 1123 (1999).